

Fluorescent speckle microscopy, a method to visualize the dynamics of protein assemblies in living cells

Clare M. Waterman-Storer*, Arshad Desai†, J. Chloe Bulinski‡ and E.D. Salmon*

Fluorescence microscopic visualization of fluorophore-conjugated proteins that have been microinjected or expressed in living cells and have incorporated into cellular structures has yielded much information about protein localization and dynamics [1]. This approach has, however, been limited by high background fluorescence and the difficulty of detecting movement of fluorescent structures because of uniform labeling. These problems have been partially alleviated by the use of more cumbersome methods such as three-dimensional confocal microscopy, laser photobleaching and photoactivation of fluorescence [2]. We report here a method called fluorescent speckle microscopy (FSM) that uses a very low concentration of fluorescent subunits, conventional wide-field fluorescence light microscopy and digital imaging with a low-noise, cooled charged coupled device (CCD) camera. A unique feature of this method is that it reveals the assembly dynamics, movement and turnover of protein assemblies throughout the image field of view at diffraction-limited resolution. We found that FSM also significantly reduces out-of-focus fluorescence and greatly improves visibility of fluorescently labeled structures and their dynamics in thick regions of living cells. Our initial applications include the measurement of microtubule movements in mitotic spindles and actin retrograde flow in migrating cells.

Addresses: *Department of Biology, University of North Carolina, Chapel Hill, North Carolina 27599-3280, USA. †Department of Cell Biology, Harvard University, Cambridge, Massachusetts, USA. ‡Cell Biology, Anatomy and Pathology, College of Physicians and Surgeons, Columbia University, New York, New York 10032-3702, USA.

Correspondence: Clare M. Waterman-Storer
E-mail: waterman@email.unc.edu

Received: 24 August 1998
Revised: 12 October 1998
Accepted: 12 October 1998

Published: 26 October 1998

Current Biology 1998, 8:1227–1230
<http://biomednet.com/elecref/0960982200801227>

© Current Biology Ltd ISSN 0960-9822

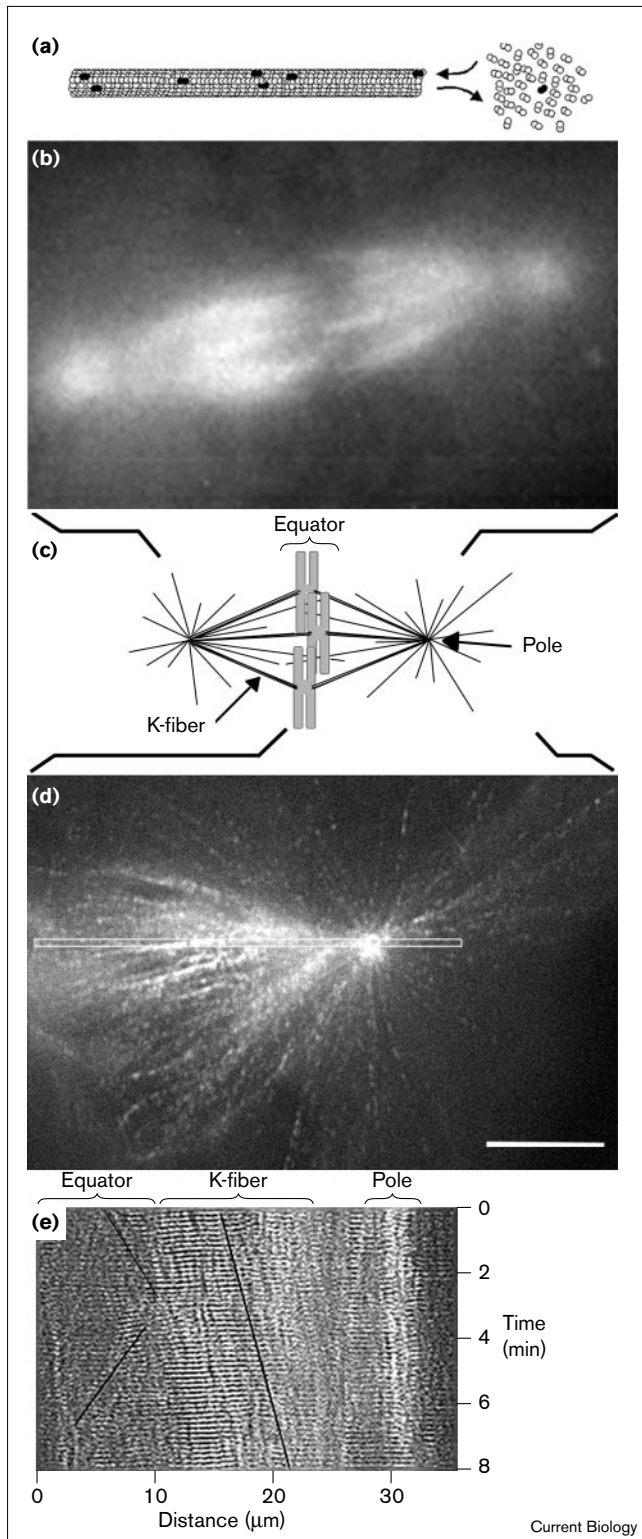
Results and discussion

In FSM, the fraction of fluorescently labeled molecules in the cell, relative to the level of endogenous unlabeled molecules, has to be very low (typically 0.5% or less). Labeled and unlabeled molecular subunits stochastically

coassemble into structures, giving a random and sparse distribution of fluorescent subunits with a ‘speckled’ appearance in high-resolution fluorescence images [3,4]. The low level of fluorescent subunits reduces background fluorescence. Translation of the fluorescent speckle distribution indicates movement of structures whereas changes in speckle intensity and pattern reveal assembly dynamics and subunit turnover. Keys to successful FSM are the ability to image diffraction limited regions (~0.25 μm) containing few (2–10) fluorophores and the capacity to inhibit photobleaching. This requires a sensitive imaging system with little extraneous background fluorescence, efficient light collection, a low noise/high quantum efficiency camera [5] and suppression of photobleaching [6]. We demonstrate applications of this method below.

Microtubules acquire a random fluorescent speckled pattern along their lattice when assembled *in vitro* from pure tubulin subunits or in living cells microinjected with very low levels of fluorescently labeled tubulin (Figure 1a) [3,7]. In Figure 1b,d we compare diffraction-limited conventional fluorescence [8] (~10% labeled tubulin) and FSM (~0.25% labeled tubulin [7]) images of the array of microtubules in mitotic spindles of living newt lung epithelial cells injected with X-rhodamine-labeled tubulin. In the conventional fluorescence image (Figure 1b), the bundles of kinetochore fiber microtubules are evident but individual astral microtubules are invisible above the high background fluorescence caused by unincorporated labeled tubulin and out-of-focus microtubule fluorescence. In the FSM image (Figure 1d), the background fluorescence is greatly reduced, and there is generally 1–3 μm between the brightest peaks in fluorescence intensity along microtubules. This increase in signal-to-noise ratio renders individual microtubules visible in both the spindle pole aster and the 5–10 μm thick spindle equator, where there are more than 1000 microtubules.

Time-lapse FSM (see Supplementary material published with this paper on the internet) showed individual astral microtubules that were growing and shortening from their free ends distal to the pole, seen as appearance and disappearance of linear arrays of fluorescent speckles. Microtubule motility within the spindle was seen as movements of microtubule fluorescent speckles. This motility can be illustrated with a kymograph analysis, in which a long thin rectangular region aligned along the axis of speckle movement (white box, Figure 1d) is extracted from each image in the time-lapse series and pasted sequentially side-by-side

**Figure 1**

FSM of microtubules in a living newt lung epithelial cell. **(a)** Schematic diagram of stochastic incorporation of labeled (black) and unlabeled (colorless) tubulin subunits into a growing microtubule. **(b,d)** Comparison of (b) conventional ($\sim 10\%$ labeled tubulin) and (d) FSM ($\sim 0.25\%$ labeled tubulin) wide-field fluorescence images, taken at the same magnification on the same imaging system, of X-rhodamine-labeled microtubules in the mitotic spindles of living cells. **(c)** Diagrammatic representation of a mitotic spindle. The portions of the spindles that are shown in the micrographs in (b,d) are highlighted by the brackets above and below the diagram, respectively. K-fiber, kinetochore fiber. The image in (d) is from a time-lapse series; the boxed region was used to form the kymograph in (e). The lines with slopes of the average velocity of microtubule movement in the spindle equator and in kinetochore fibers are highlighted by black lines across that region of the kymograph. Bar = $10\ \mu\text{m}$.

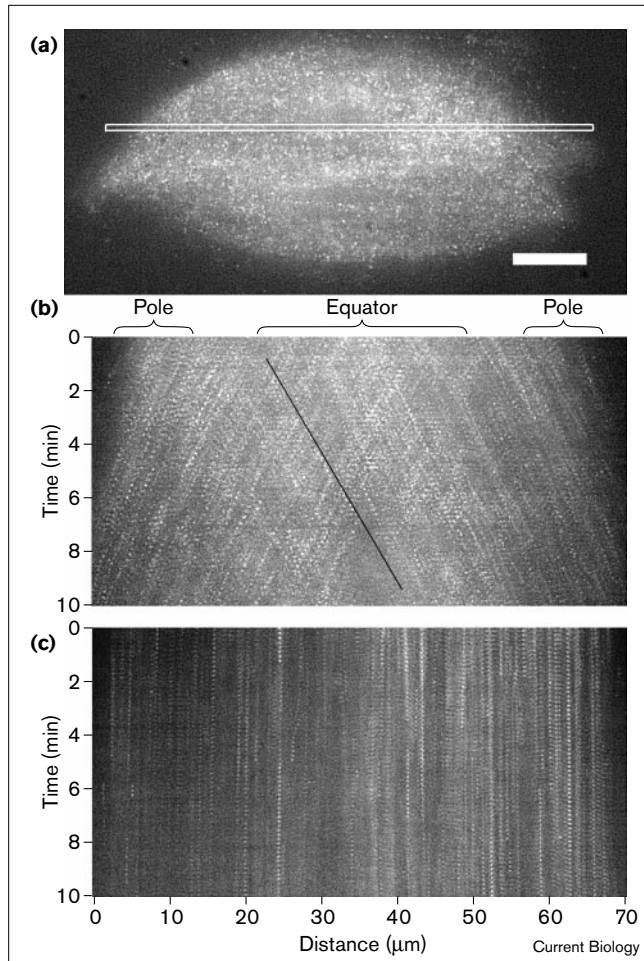
poles at the spindle equator, indicating that overlapping arrays of microtubules moved towards opposite poles at a rate of $1.63 \pm 0.49\ \mu\text{m}/\text{min}$ ($n = 18$). This analysis also shows that microtubules within kinetochore fibers move poleward at a rate of $0.75 \pm 0.2\ \mu\text{m}/\text{min}$ ($n = 16$), similar to velocities determined from lower resolution fluorescence photoactivation marking [8]. We found no evidence of similar poleward movement of astral microtubule speckles.

We have also used FSM to monitor microtubule dynamics in mitotic spindles assembled *in vitro* in *Xenopus* egg extracts [9]. Tetramethylrhodamine-labeled tubulin was added to extracts at a final concentration of $5\ \text{nM}$, equal to $\sim 0.025\%$ of the $\sim 20\text{--}30\ \mu\text{M}$ tubulin pool in the extracts [10] (Figure 2a). Time-lapse FSM of spindles assembled *in vitro* revealed a continuous flux of microtubule speckles towards opposite spindle poles, where speckles disappear as microtubules depolymerize at a constant rate (see Supplementary material). Kymograph analysis of the time-lapse sequence showed slow spindle elongation of $\sim 1\ \mu\text{m}/\text{min}$ and more rapid poleward microtubule flux throughout each half spindle at $\sim 2\ \mu\text{m}/\text{min}$. This is similar to rates of poleward microtubule flux measured by low-resolution fluorescence photoactivation methods [9]. Poleward microtubule movement is stopped by the addition of the non-hydrolyzable analog of ATP, AMP-PNP, at $1.5\ \text{mM}$ (Figure 2c), which is thought to inhibit an unknown microtubule-based motor protein [9]. In contrast to fluorescently labeled tubulin, FSM of the microtubule-binding domain of the microtubule-binding protein ensconsin [11], ligated to multiple copies of green fluorescent protein and expressed at low levels in cultured monkey TC-7 cells, revealed rapid binding and release of fluorescent ensconsin from microtubules (data not shown).

to make a montage of the region over time (Figure 1e). In these kymographs, oblique white streaks correspond to the movement of bright microtubule speckles over time, with the slopes of the streaks related to the velocity of speckle movement. Kymographs along the spindle axis revealed the movement of microtubules towards opposite spindle

FSM can also be used to examine the motility and assembly dynamics of actin filament arrays in migrating epithelial cells. As with microtubules, low levels of incorporation of X-rhodamine-labeled actin subunits into actin filaments (Figure 3a) give a speckled appearance to actin filaments

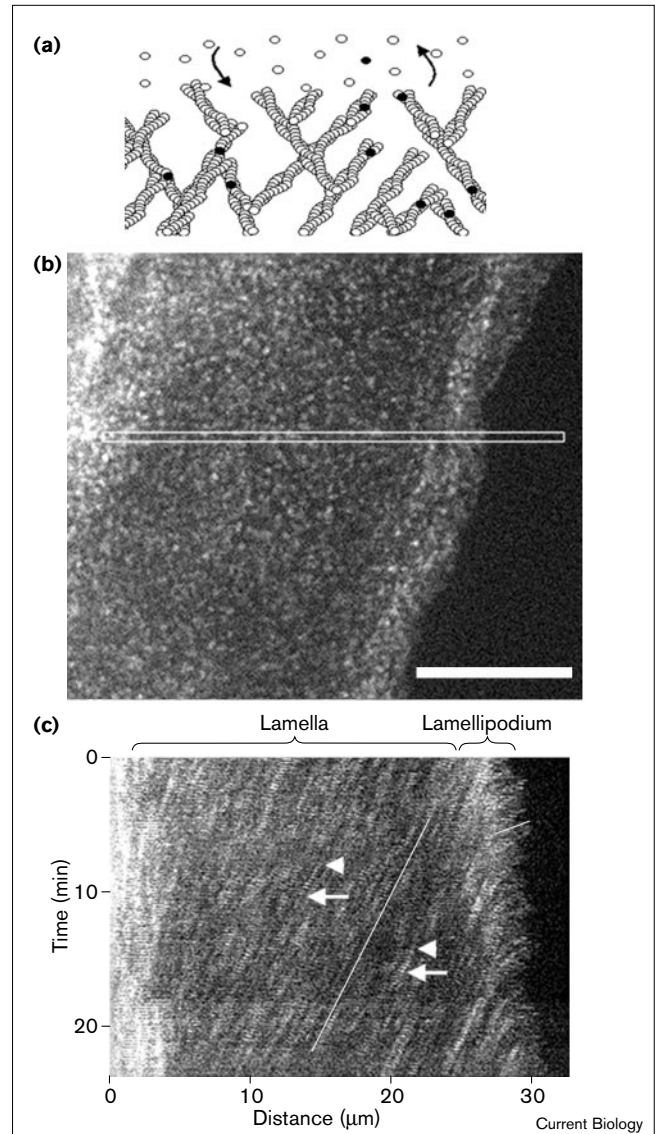
Figure 2



FSM of microtubules in mitotic spindles assembled *in vitro* in *Xenopus laevis* egg extracts. **(a)** FSM image from a time-lapse sequence of tetramethylrhodamine-labeled tubulin in an *in vitro* assembled mitotic spindle. The boxed area in (a) in each image in the time-lapse series was used to create the kymograph in **(b)**. A line with the slope of the average velocity of microtubule poleward flux and spindle elongation ($3.2 \mu\text{m}/\text{min}$) is highlighted by a black line in **(b)**. The kymograph in **(c)** was constructed from a similar region of a spindle with similar dimensions as that in (a), except that the extract was treated with 1.5 mM AMP-PNP . Bar = $10 \mu\text{m}$.

in vitro [4] and to the lamellipodia lamella region when microinjected into a living cell (Figure 3b). Time-lapse sequences (see Supplementary material) of actin FSM images and kymographs of speckle movement revealed that actin moves rearward in lamellipodia at the leading edge of migrating cells at a rate of $1.61 \pm 0.42 \mu\text{m}/\text{min}$ ($n = 16$), similar to previous reports using different methods [12,13], and more slowly ($0.40 \pm 0.22 \mu\text{m}/\text{min}$, $n = 22$) in proximal regions of the lamella (Figure 3c). Kymograph analysis along the axis of actin movement also showed the appearance of fluorescent speckles (arrowheads, Figure 3c), indicating that labeled actin has incorporated into the lamella meshwork, and disappearance of

Figure 3



FSM of actin in a migrating newt lung epithelial cell. **(a)** Schematic diagram of incorporation of labeled (black) and unlabeled (colorless) actin subunits into an actin filament meshwork. **(b)** FSM image from a time-lapse sequence of X-rhodamine-labeled actin in the lamella of a cell migrating to the right. The area boxed in (b) along the axis of speckle movement was used to create the kymograph in **(c)**. Lines with slopes of the average velocities of retrograde actin movement in the lamellipodia and lamella are highlighted by a white line across that region of the kymograph. Appearance (arrowheads) and disappearance (arrows) of speckles in the kymograph indicates the incorporation and disassembly, respectively, of F-actin in the lamella. Bar = $10 \mu\text{m}$.

speckles (arrows, Figure 3c), indicating actin depolymerization. This demonstrates that FSM will be useful for measuring the turnover of actin polymers in nearly two-dimensional arrays of filamentous actin (F-actin), such as those in the lamella and lamellipodia, where vertical

movement of actin into or out of the plane of focus should not contribute to speckle appearance or disappearance.

Our results demonstrate that FSM offers for the first time the optical clarity needed to achieve detailed analyses of polymer dynamics within dense arrays such as the mitotic spindle and cortical actin cytoskeleton, obviating the need for photoactivation and photobleaching methods. FSM should be useful for a wide variety of fluorescently labeled molecules in many sub-cellular structures and macromolecular assemblies.

Materials and methods

Preparation, microinjection and expression of fluorescently labeled proteins in living cells and cell extracts

Porcine brain tubulin was purified and conjugated to X-rhodamine or tetramethylrhodamine to a dye-to-protein ratio of 1.2–1.4:1 [14]. Chicken breast muscle actin was purified from acetone powder and conjugated to X-rhodamine succinimidyl ester [15]. Newt lung epithelial cells [7] were pressure microinjected with X-rhodamine-labeled proteins at a needle concentration of 1 mg/ml and mounted in media containing 0.3–0.6 units/ml of the oxygen scavenging enzyme Oxyrase (Oxyrase Inc.) [6]. CSF-arrested extracts of *Xenopus laevis* eggs were prepared and cycled spindle assembly was performed as described [9]. Tetramethylrhodamine-labeled tubulin was added to the extract at a final concentration of 5 nM [9]. The cDNA encoding the microtubule-binding region of human ensconsin was inserted into the eGFPn-1 vector (Clontech) such that eGFP was fused to the 3' end. This construct was transfected into TC-7 cells and stably transformed cells were selected by G418 resistance.

Image acquisition

Digital fluorescence images of living cells were acquired using the multi-mode fluorescence microscope system previously described [5]. This consists of a Nikon Microphot FXA equipped with a 60 \times , 1.4 NA Plan Apo DIC objective, 1.25 body tube magnifier, 1.5 \times projection magnifier to the camera and epi-illumination provided by a HBO100 mercury arc lamp. Fluorescence images were collected with a Hamamatsu C-4880 CCD camera containing a TC215 chip cooled to -30°C , which has 12 μm square pixels and a 12 bit linear range of photon detection [5]; 1–2 sec exposures of microtubules and actin were acquired at 10 sec and 15 sec intervals, respectively. Digital fluorescence images of *Xenopus* egg extracts were acquired with a Nikon E800 microscope equipped with a 60 \times , 1.4 NA Plan Apo DIC infinity corrected objective, epifluorescence illumination provided by an HBO-100 W mercury arc lamp and a HiQ TRITC filter set (Chroma). Images were acquired at 10 sec intervals using 1 sec exposure on a Princeton Instruments TEA/CCD-1317-K/1 camera equipped with a 12 bit Kodak KAF1400 CCD chip with 6.9 μm square pixels and cooled to -40°C .

Image processing and data analysis

All image processing and analysis was performed using functions in the MetaMorph software. To correct for camera defects, 25 1–2 sec 'background' images were acquired with light to the camera shuttered. These background images were averaged and subtracted from each image in the time-lapse series. To correct for differences in illumination intensity, the images were 'equalized' by choosing a reference area in the background of one image, averaging the pixel intensities in that area and setting the average of the corresponding area of all other images in the series equal to the reference average. To enhance fluorescent speckles, an 'unsharp mask' routine was used by applying a 9×9 low pass filter to each image, multiplying the low-passed images by 0.5, subtracting from the original images and scaling the result to restore the contrast range. Pixel-to-distance conversion factors were determined from images of a 10 μm stage micrometer. To determine

rates of microtubule translocation in mitotic spindles in living cells, images were aligned relative to the position of the centrosome in the first image in the series using the 'align stack' function in MetaMorph. Individual speckles were tracked using the 'track points' function, and values were exported to Microsoft Excel for determination of speckle velocity. Movement of both actin and microtubule speckles was also analyzed by constructing kymographs. The time-lapse series was first examined as a movie to determine the trajectory of speckle movement. In the kymographs, the movements of speckles appear as bright oblique streaks, the slope of which correspond to the velocity of microtubule or actin movement.

Supplementary material

Quicktime movies of the time-lapse speckle images accompanying Figures 1–3 are published with this article on the internet and are also available at <http://www.unc.edu/depts/salmlab/salmmov.html>.

Acknowledgements

We thank Mike Caplow, Tim Mitchison and Ken Jacobsen. C.M.W-S. is supported by a fellowship from the Jane Coffin Childs Memorial Fund for Cancer Research. This work was supported by NIH GMS 24364 to E.D.S and NCI CA-70951 to J.C.B.

References

1. Wang YL: **Fluorescent analog cytochemistry: tracing functional protein components in living cells.** *Methods Cell Biol* 1989, **29**:1-12.
2. Sluder G, Wolf DE (editors): **Video microscopy.** *Methods in Cell Biology*, vol 56; 1998.
3. Waterman-Storer CM, Salmon ED: **How microtubules get fluorescent speckles.** *Biophys J* 1998, **75**:2059-2069.
4. Sase I, Miyata H, Corrie JET, Craik JS, Kinoshita K Jr: **Real time imaging of single fluorophores on moving actin with an epifluorescence microscope.** *Biophys J* 1995, **69**:323-328.
5. Salmon ED, Shaw SL, Waters J, Waterman-Storer CM, Maddox PS, Yeh E, Bloom K: **A high resolution multi-mode digital microscope system.** *Methods Cell Biol* 1998, **56**:185-214.
6. Waterman-Storer CM, Sanger JW, Sanger JM: **Dynamics of organelles in the mitotic spindles of living cells: membrane and microtubule interactions.** *Cell Motil Cytoskeleton* 1993, **26**:19-39.
7. Waterman-Storer CM, Salmon ED: **Actomyosin-based retrograde flow of microtubules in the lamella of migrating epithelial cells influences microtubule dynamic instability and turnover and is associated with microtubule breakage and treadmilling.** *J Cell Biol* 1997, **139**:417-434.
8. Waters JC, Mitchison TJ, Rieder CL, Salmon ED: **The kinetochore microtubule minus-end disassembly associated with poleward flux produces a force that can do work.** *Mol Biol Cell* 1996, **7**:1547-5158.
9. Desai A, Maddox PS, Mitchison TJ, Salmon ED: **Anaphase A chromosome movement and poleward spindle microtubule flux occur at similar rates in *Xenopus* extract spindles.** *J Cell Biol* 1998, **141**:703-713.
10. Parsons SF, Salmon ED: **Microtubule assembly in clarified *Xenopus* egg extracts.** *Cell Motil Cytoskeleton* 1997, **36**:1-11.
11. Bulinski JC, Bossler A: **Purification and characterization of ensconsin, a novel microtubule stabilizing protein.** *J Cell Sci* 1994, **107**:2839-2849.
12. Theriot JA, Mitchison TJ: **Comparison of actin and cell surface dynamics in motile fibroblasts.** *J Cell Biol* 1992, **119**:367-377.
13. Wang YL: **Exchange of actin subunits at the leading edge of living fibroblasts: possible role of treadmilling.** *J Cell Biol* 1985, **101**:597-602.
14. Hyman A, Drechsel D, Kellogg D, Salser S, Sawin K, Steffen P, et al.: **Preparation of modified tubulins.** *Meth Enzymol* 1991, **196**:478-485.
15. Turnacioglu KK, Sanger JW, Sanger JM: **Sites of monomeric actin incorporation in living PtK2 and REF-52 cells.** *Cell Motil Cytoskeleton* 1998, **40**:59-70.

Fluorescent speckle microscopy, a method to visualize the dynamics of protein assemblies in living cells

Clare M. Waterman-Storer, Arshad Desai, J. Chloe Bulinski and E.D. Salmon
Current Biology 26 October 1998, **8**:1227–1230

Movies

Quick-time movies of the time-lapse speckle images in Figures 1–3 are shown.